THE JOURNAL OF BIOLOGICAL CHEMISTRY VOL. 287, NO. 10, pp. 7411–7426, March 2, 2012
© 2012 by The American Society for Biochemistry and Molecular Biology, Inc. Published in the U.S.A.

CHCM1/CHCHD6, Novel Mitochondrial Protein Linked to Regulation of Mitofilin and Mitochondrial Cristae Morphology*[S]

Received for publication, July 15, 2011, and in revised form, January 4, 2012 Published, JBC Papers in Press, January 6, 2012, DOI 10.1074/jbc.M111.277103

Jie An, Jingxue Shi, Qin He, Ki Lui, Yuxin Liu, Ying Huang, and M. Saeed Sheikh[1]

From the Department of Pharmacology, State University of New York, Upstate Medical University, Syracuse, New York 13210

Background: Functional characterization of a novel mitochondrial protein, CHCM1/CHCHD6, is reported.
Results: CHCM1 interacts with Mitofilin, DISC1, and CHCHD3, and its deficiency leads to severe defects in mitochondrial cristae morphology, reduction in cell growth, ATP production, and oxygen consumption.
Conclusion: CHCM1/CHCHD6 is a novel player linked to mitochondrial cristae morphology.
Significance: Results provide valuable insights into molecular events controlling the structural integrity and biogenesis of mitochondrial cristae.

The structural integrity of mitochondrial cristae is crucial for mitochondrial functions; however, the molecular events controlling the structural integrity and biogenesis of mitochondrial cristae remain to be fully elucidated. Here, we report the functional characterization of a novel mitochondrial protein named CHCM1 (coiled coil helix cristae morphology 1)/CHCHD6. CHCM1/CHCHD6 harbors a coiled coil helix-coiled coil helix domain at its C-terminal end and predominantly localizes to mitochondrial inner membrane. CHCM1/CHCHD6 knockdown causes severe defects in mitochondrial cristae morphology. The mitochondrial cristae in CHCM1/CHCHD6-deficient cells become hollow with loss of structural definitions and reduction in electron-dense matrix. CHCM1/CHCHD6 depletion also leads to reductions in cell growth, ATP production, and oxygen consumption. CHCM1/CHCHD6 through its C-terminal end strongly and directly interacts with the mitochondrial inner membrane protein mitofilin, which is known to also control mitochondrial cristae morphology. CHCM1/CHCHD6 also interacts with other mitofilin-associated proteins, including DISC1 and CHCHD3. Knockdown of CHCM1/CHCHD6 reduces mitofilin protein levels; conversely, mitofilin knockdown leads to reduction in CHCM1 levels, suggesting coordinate regulation between these proteins. Our results further indicate that genotoxic anticancer drugs that induce DNA damage down-regulate CHCM1/CHCHD6 expression in multiple human cancer cells, whereas mitochondrial respiratory chain inhibitors do not affect CHCM1/CHCHD6 levels. CHCM1/CHCHD6 knockdown in human cancer cells enhances chemosensitivity to genotoxic anticancer drugs, whereas its overexpression increases resistance. Collectively, our results indicate that CHCM1/CHCHD6 is linked to regulation of mitochondrial cristae morphology, cell growth, ATP production, and oxygen consumption and highlight its potential as a possible target for cancer therapeutics.

Mitochondria are key organelles that contain double membranes and harbor their own DNA as well as components of transcriptional and translational machinery. They are implicated in a variety of processes, including energy or free radical generation, regulation of apoptosis, and modulation of various signaling pathways. Defects in mitochondrial function have been associated with a variety of pathological states, including but not limited to neurogenic muscle weakness, ataxia and retinitis pigmentosa, mitochondrial encephalomyopathy, lactic acidosis, and stroke-like episodes, myoclonic epilepsy and ragged-red fibers, Leber hereditary optic neuropathy; and Kearns-Sayre syndrome (1, 2). There is also a strong link between alterations in mitochondrial function and a variety of cancers (1, 3–5).

Mitochondria are dual membrane organelles that contain an outer membrane and an inner membrane. Although several models of mitochondrial inner membrane topology have been proposed, it is generally believed that within the inner membrane there exist an inner boundary membrane and the cristae membrane (6). The inner boundary membrane is believed to be in closer proximity of the outer membrane, whereas the cristae membrane extends into the mitochondrial matrix, and these membranes are joined via cristae junctions. Thus, the mitochondrial cristae are formed by the inner membrane folds extending as invaginations (6). Although the exact molecular mechanisms of how mitochondrial cristae and cristae junctions are formed are not understood, emerging evidence suggests that the integrity of mitochondrial cristae morphology is important for mitochondrial structure and function. For example, mitochondrial cristae remodeling has been proposed to affect mitochondrial storage and release of cytochrome *c* (7–9). It has also been proposed that OPA1 and Parl play an important role in regulation of cristae remodeling (7–9). Other proteins, including mitofilin, MICS1, F_1F_0-ATP synthase, DISC1, and CHCHD3, have also been reported to be involved in regulation

* This work was supported, in whole or in part, by National Institutes of Health Grants CA157168 and ES016668 (to M. S. S.).
The nucleotide sequence(s) reported in this paper has been submitted to the GenBank™/EBI Data Bank with accession number(s) JF264889.
[S] This article contains supplemental Figs. 1 and 2.
[1] To whom correspondence should be addressed: SUNY Upstate Medical University, 750 E. Adams St., Syracuse, NY 13210. Tel.: 315-464-8015; Fax: 315-464-8014; E-mail: sheikhm@upstate.edu.

of mitochondrial cristae morphology (10–14). The molecular mechanisms that control the structural integrity and biogenesis of mitochondrial cristae remain to be fully elucidated, and identification of additional molecules is expected to greatly improve the understanding of these events.

In this paper, we report the identification and characterization of a novel mitochondrial protein that we have named CHCM1 (coiled coil helix cristae morphology 1) that is also linked to controlling mitochondrial cristae structures. Sequence corresponding to CHCM1 was found to be annotated in the database as a hypothetical protein, CHCHD6, without experimental characterization. Our results indicate that the presence of CHCM1 (hereafter referred to as CHCM1/CHCHD6) is critical for maintaining the mitochondrial cristae morphology, ATP production, and oxygen consumption. CHCM1/CHCHD6 predominantly localizes to the mitochondrial inner membrane and strongly interacts with mitofilin, another mitochondrial inner membrane protein. CHCM1/CHCHD6 is regulated in response to DNA damage (genotoxic stress), and alterations in its expression affect chemosensitivity of human cancer cells to genotoxic anticancer drugs.

EXPERIMENTAL PROCEDURES

Cell Culture, Antibodies, and Reagents—Cell lines HEK293T (human embryonic kidney cells), MCF7 (human breast cancer cells), RKO (human colon cancer cells), MDA231 (human breast cancer cells), MDA468 (human breast cancer cells), Hs578T (human breast cancer cells), UACC-62 (human melanoma cells), and SK-Mel-103 (human melanoma cells) were maintained in Dulbecco's modified Eagle's medium (DMEM) supplemented with 10% fetal bovine serum (Gemini Bio-Products Inc., West Sacramento, CA). Human breast cancer cell line BT549 was maintained in RPMI 1640 medium supplemented with 10% fetal bovine serum. The following antibodies were used in our studies: anti-HA tag (clone 3F10) (Roche Applied Science), anti-β-actin (Sigma-Aldrich), anti-VDAC1 (Calbiochem, EMD Chemicals Group, Darmstadt, Germany), anti-mitofilin (Protein Tech Group, Chicago, IL), anti-p97 (Fitzgerald Industries International, Concord, MA), anti-Tim23 (BD Biosciences), anti-S-tag (Novagen, EMD Biosciences, Darmstadt, Germany), anti-GST (GenScript, Piscataway, NJ), anti-Hsp60 (Enzo Life Sciences, Plymouth Meeting, PA), anti-Smac (Upstate Cell Signaling Solutions, Lake Placid, NY), anti-CHCHD3 (Abcam, San Francisco, CA), and anti-DISC1 (Santa Cruz Biotechnology, Inc., Santa Cruz, CA). Rabbit polyclonal antibodies specific for human CHCM1/CHCHD6 were generated in our laboratory through a commercial source (ProSci Inc., Poway, CA) using full-length recombinant human CHCM1/CHCHD6 protein purified from *Escherichia coli*. For cell transfections, Lipofectamine 2000 (Invitrogen) was used. Restriction endonucleases for subcloning were from New England BioLabs (Ipswich, MA). *Pfu* DNA polymerase was from Stratagene (La Jolla, CA). Chemical reagents used in transmission electron microscopy experiments were from Electron Microscopy Sciences (Hatfield, PA) and Polysciences Inc. (Warrington, PA). Other chemical reagents were from Thermo Fisher Scientific and Sigma-Aldrich.

Expression Constructs—Clones containing cDNAs of CHCM1/CHCHD6 and mitofilin were purchased from ATCC (Manassas, VA) and Open Biosystems (Huntsville, AL), respectively. Fragments corresponding to open reading frames (ORFs) of CHCM1/CHCHD6, mitofilin, and CHCM1/CHCHD6 deletion variants were generated by PCR amplification. ORF of CHCM1/CHCHD6 and its deletion variants were inserted into pSRα-HA-S and pET30a (Novagen) expression vectors, respectively. HA-S-tagged CHCM1/CHCHD6-pcDNA3.1 expression construct was obtained by inserting CHCM1/CHCHD6 ORF into pcDNA3.1 mammalian expression vector (Invitrogen). GST-tagged mitofilin was generated by inserting ORF of mitofilin into pGEX6P-1 expression vector (GE Healthcare). All vectors were sequenced to validate their authenticity.

Stable Transfection—For stable transfections, expression vector pcDNA3.1 carrying HA/S-tagged CHCM1/CHCHD6 was used. The same vector without the CHCM1/CHCHD6 insert was used for control transfection. RKO human colon cancer cells were transfected with these vectors using Lipofectamine 2000 (Invitrogen), and G418-resisitant colonies were selected after ~2 weeks. Several independent colonies were picked up and expanded into mass culture and screened for the expression of exogenous CHCM1/CHCHD6. Several vector-only transfected colonies were also isolated, pooled, and expanded into mass culture. CHCM1/CHCHD6-expressing clones B4, C3, and C4 were selected for further studies.

Immunostaining—Immunostaining of exogenous CHCM1/CHCHD6 tagged with HA was performed as described previously with some modifications (15). Briefly, cells were cultured in Lab-tek II chamber slides and then transiently co-transfected with pSRα-HA expression vector alone or CHCM1/CHCHD6-HA-pSRα expression construct with pDsRed2-Mito (Clontech, Mountain View, CA), respectively. After ~24 h, cells were fixed with 4% paraformaldehyde for 30 min, followed by methanol (−20 °C) for 10 min and acetone (−20 °C) for 10 s. Then anti-HA primary antibody and FITC-conjugated secondary antibody (Jackson ImmunoResearch Laboratories, West Grove, PA) were used to label cells. Nuclear staining was with DAPI nuclear dye. Slides were observed under an Olympus fluorescent microscope using the appropriate filters.

Immunostaining of endogenous CHCM1/CHCHD6 was performed as described previously with minor modifications (16). Briefly, cells were cultured in Lab-tek II chamber slides and stained with MitoTracker® according to the manufacturer's protocols (Molecular Probes/Invitrogen). Then cells were fixed with 4% paraformaldehyde for 30 min and incubated with PBS buffer for 5 min and PBS plus 0.1% Triton X-100 buffer for 10 min. Later cells were subjected to an incubation for 1 h with PBS plus 1% BSA and 0.05% Triton X-100 buffer at room temperature. Finally, cells were incubated with normal rabbit IgG alone or anti-CHCM1/CHCHD6 primary antibody diluted (1:600) in PBS plus 0.05% Triton X-100 buffer, respectively, at 4 °C overnight. The next day, cells were washed with PBS plus 1% BSA buffer three times for 10 min each. Then, as a secondary antibody, FITC-conjugated anti-rabbit antibody was employed; DAPI was used for nuclear staining, and slides were analyzed

using an Olympus fluorescent microscope that had the required filters.

Isolation and Fractionation of Mitochondria—Isolation and fractionation of mitochondria were performed according to standard procedures (17). Briefly, cells were harvested by 600 × *g* centrifugation for 10 min. After washing with cold PBS once, cells were resuspended with 5 volumes of homogenization buffer (0.25 M sucrose, 20 mM HEPES-KOH, pH 7.5, 10 mM KCl, 1.5 mM $MgCl_2$, 1 mM EDTA, 1 mM EGTA, 1 mM dithiothreitol, and 0.1 mM PMSF). The suspension was subsequently homogenized with a Dounce glass homogenizer, and the mixture was centrifuged at 750 × *g* at 4 °C for 15 min. Supernatant was collected and centrifuged at 10,000 × *g* at 4 °C for 15 min. The pellet was obtained, which represented crude mitochondria, and the supernatant was further centrifuged at 100,000 × *g* for 1 h to obtain the cytosolic fraction.

Submitochondrial Fractionations—RKO human colon cancer cells were used for generating submitochondrial fractions. Mitochondria from these cells were isolated and gradient-purified as described previously (18). Briefly, cells were harvested by low speed centrifugation and resuspended in homogenization buffer (10 mM NaCl, 1.5 mM $MgCl_2$, and 10 mM Tris-HCl, pH 7.5). The suspension was incubated on ice for 4–5 min, homogenized in a Dounce glass homogenizer, and subsequently transferred to sucrose-containing $T_{10}E_{20}$ buffer (10 mM Tris-HCl, 1 mM EDTA, pH 7.6) with final sucrose concentration at 250 mM. After centrifugation at 1300 × *g* for 3 min, supernatant was isolated and centrifuged at 1300 × *g* for an additional 3 min. The supernatant was further centrifuged at 15,000 × *g* for 15 min, and crude mitochondria were portioned in the pellet fraction. The crude mitochondrial fraction was washed three times with 250 mM sucrose in $T_{10}E_{20}$ buffer and layered on a discontinuous sucrose gradient (1.0 and 1.7 M sucrose in $T_{10}E_{20}$ buffer) and centrifuged at 70,000 × *g* for 40 min. The mitochondrial fraction from the interface between two layers was recovered and diluted with an equal volume of 250 mM sucrose in $T_{10}E_{20}$ buffer, and purified mitochondria were obtained after 15,000 × *g* centrifugation for 15 min.

To prepare mitochondrial subfractionations, we used the swell-contract method as reported previously (19, 20). Briefly, purified mitochondria were suspended in 20 mM potassium phosphate (pH 7.2) containing 0.02% BSA on ice for 20 min; ATP and $MgCl_2$ were then added at a final concentration of 1 mM and incubated on ice for an additional 5 min. The mixture was centrifuged at 10,000 × *g* for 10 min, and the recovered pellet was resuspended in suspension buffer (0.25 M sucrose, 1 mM EGTA, and 10 mM HEPES-NaOH, pH 7.4) and centrifuged at 10,000 × *g* for 10 min to recover mitoplasts in the pellet fraction. All supernatants were collected and centrifuged at 100,000 × *g* for 1 h. The final supernatant represented the intermembrane space fraction, and the pellet fraction corresponded to the outer membrane fraction. The mitoplast fraction was resuspended in suspension buffer without BSA, and an equal volume of lysis buffer (25 mM HEPES, pH 7.0, containing 1% Triton X-100) was added. The mixture was incubated on ice for 30 min and finally centrifuged at 100,000 × *g* for 1 h to recover the matrix fraction in the supernatant and the inner membrane fraction in the pellet.

Sodium Carbonate Extraction Assay—The sodium carbonate extraction assay was performed according to previously published reports (21, 22). Briefly, RKO or MCF-7 cells were homogenized with a Dounce glass homogenizer in a buffer composed of 250 mM sucrose, 10 mM Tris-HCl, pH 7.4, 1 mM DTT, 1 mM EDTA, and protease inhibitors, and the mixture was centrifuged at 100,000 × *g* for 1 h to separate membrane and soluble fractions. Then about 60 μg of membrane proteins were diluted 50-fold in 100 mM sodium carbonate (pH 11.5) and incubated on ice for 30 min. The suspension was centrifuged 240,000 × *g* for 1 h at 4 °C. The membrane-associated fraction portioned in the supernatant was precipitated with trichloroacetic acid (TCA), whereas the pellet representing the membrane integral fraction was dissolved in 1× protein loading buffer.

Northern Blot Analyses—Northern blot analyses were done according to standard procedure (23, 24). Briefly, total RNA was extracted by TRIzol reagent (Invitrogen), and ~15 μg of total RNA were size-separated on 1.2% agarose gel and transferred to nylon membrane (Whatman, GE Healthcare). Human CHCM1/CHCHD6 cDNA probe was labeled with ^{32}P, and hybridization was performed in QuikHyb solution (Stratagene, La Jolla, CA) at 65 °C.

Western Blotting, S-tag Pull-down, and Immunoprecipitation—Western blotting and immunoprecipitations were done by standard procedures as we have described previously (25, 26). S-tag pull-down experiments were performed using human cancer cells as well as bacterial lysates. Cell pellets were prepared and lysed in lysis buffer (50 mM Tris-HCl, pH 7.4, 120 mM NaCl, 0.1% Nonidet P-40, 10 mM NaF, 5 mM EDTA, 2 mM Na_3VO_4, 2 mM $MgCl_2$, 10 mM KCl, 25 mM glycerophosphate, protease inhibitor mixture, okadaic acid, and 1 mM PMSF), and S-tag pull-down was performed by using S-protein-agarose beads (Novagen) according to the manufacturer's protocol. For S-tag pull-down using bacterial lysates, wild type and deletion variants of S-tagged CHCM1/CHCHD6 were expressed in *E. coli* BL21 (DE3) and induced by 1 mM isopropyl-1-thio-β-D-galactopyranoside at 30 °C for 6 h. Bacteria were lysed in a buffer containing 28 mM Tris, 135 mM NaCl, 1 mM dithiothreitol (DTT), 1% Triton X-100 (w/v), protease inhibitor mixture, and 400 μg/ml lysosome for 30 min at room temperature, followed by 26,000 × *g* centrifugation for 30 min (Sorvall RC5C Plus), and S-tag pull-down was done according to the manufacturer's protocol. GST-tagged mitofilin was expressed in bacteria and gel-purified as described previously (27).

RNA Interference (RNAi)—Endogenous CHCM1/CHCHD6 and mitofilin were knocked down by a lentiviral shRNA-mediated approach (28). The pLKO.1 lentiviral vectors containing the scrambled or CHCM1/CHCHD6-specific shRNAs or mitofilin-specific shRNAs were generated by the RNA Interference Consortium and purchased from Open Biosystems (Huntsville, AL). Lentivirus were produced and titered according to the supplier's protocols. In all experiments, the multiplicity of infection was 1.0. The following five shRNAs to target five different regions of CHCM1/CHCHD6 were used (the first part of the sequence is in sense orientation and then loop (underlined) followed by antisense sequence): CHCM1/CHCHD6-specific shRNA-G4, GAGCGTATTGAGAGG-

AAGAATCTCGAGATTCTTCCTCTCAATACGCTCT; CHCM1/CHCHD6-specific shRNA-G5, CCTGAAGAAGGGACCAATCATCTCGAGATGATTGGTCCCTTCTTCAGGT; CHCM1/CHCHD6-specific shRNA-G6, GCATGCTGCTATCCAGGATAACTCGAGTTATCCTGGATAGCAGCATGCT; CHCM1/CHCHD6-specific shRNA-G7, CTTTGGCCTTCAAGATGGCAACTCGAGTTGCCATCTTGAAGGCCAAAGT; CHCM1/CHCHD6-specific shRNA-G8, GCTGAGATGTATAAACTGTCTCTCGAGAGACAGTTTATACATCTCAGCT. The following four shRNAs to target four different regions of mitofilin were used (first part of the sequence is in sense orientation and then loop (underlined) followed by antisense sequence): mitofilin-specific shRNA-A1, CCGGGCTAAGGTTGTATCTCAGTATCTCGAGATACTGAGATACAACCTTAGCTTTTTTG; mitofilin-specific shRNA-A2, CCGGCCAAGCTTTAACCGCAGCTATCTCGAGATAGCTGCGGTTAAAGCTTGGTTTTTTG; mitofilin-specific shRNA-A3, CCGGGCACTATCCTATATGCCAAATCTCGAGATTTGGCATATAGGATAGTGCTTTTTTG; mitofilin-specific shRNA-A4, CCGGGTCTAGAAATGAGCAGGTTTACTCGAGTAAACCTGCTCATTTCTAGACTTTTTTG.

MTT[2] Assay—MTT powder was dissolved in DMEM without fetal bovine serum and phenol red to a final concentration of 1 mg/ml and then added to cells and incubated for ~1–4 h, depending on cell confluence. Medium was then removed, and an equal volume of isopropyl alcohol with 0.04 N HCl was added to dissolve the precipitate. Finally, absorbance was read at the 570-nm wavelength subtracting background reading at the 650-nm wavelength with a Bio-Rad SmartSpec 3100 instrument.

Transmission Electron Microscopy—Scramble and CHCM1/CHCHD6 knockdown cells were harvested and fixed by Ito and Karnovsky's fixative (2.5% glutaraldehyde, 2% paraformaldehyde in 0.1 M cacodylate buffer, pH 7.4) at 4 °C overnight (29). The next day, cells were rinsed with 0.1 M cacodylate buffer five times for 5 min each. After fixing with 1% osmium tetroxide in 0.1 M cacodylate buffer for 1 h on ice, the samples were rinsed with double-distilled H_2O three times for 8 min each and later fixed with 1% tannic acid for 1 h. After rinsing with double-distilled H_2O an additional three times for 8 min each, samples were dehydrated and embedded into Poly/Bed® 812 according to the protocol of the Poly/Bed® 812 BDMA minikit (Polyscience, Inc., Warrington, PA). Poly/Bed®-embedded cells were cut into 80–90-nm ultrathin serial sections by a diamond knife, DIATOME 45 Degrees (Diatome US, Hatfield, PA). Sections were supported on nickel grids/200-mesh (Electron Microscopy Sciences, Hatfield, PA) and poststained in 4% uranyl acetate and 4% lead citrate. Finally, sections were observed under a Tecnai™ transmission electron microscope (BioTwin lens) with an Advantage Plus CCD Camera System at an 80.0-kV acceleration voltage.

Mitochondrial ATP Synthesis Assay—The mitochondrial ATP synthesis assay was performed as reported previously (30). Briefly, CHCM1/CHCHD6 knockdown or scramble knockdown RKO cells were harvested and washed with glucose-free, serum-free DMEM. Each sample with ~1.5×10^6 cells was resuspended and incubated in 160 μl of buffer A (150 mM KCl, 25 mM Tris-HCl, 2 mM EDTA, 0.1% BSA, 10 mM potassium phosphate, pH 7.4, 0.1 mM $MgCl_2$) with digitonin (40 μg/ml final concentration) for 1 min at room temperature. After a wash with buffer A, cells were centrifuged at 800 $\times$ *g* at room temperature, and pellets were resuspended in 160 μl of buffer A containing P^1, P^5-di(adenosine) pentaphosphate (0.15 mM). Subsequently, 10 μl of buffer B (0.5 M Tris acetate, pH 7.75, 0.8 mM luciferin, 20 μg/ml luciferase), ADP (to 0.1 mM), and malate and pyruvate (both to 1 mM) were added to the cell suspension. Oligomycin (1 μg/ml) was also added to one replicate of each sample prepared as above. Cells were transferred to luminometer glass tubes and gently mixed with a vortex for 2 s. Tubes were then placed in a luminometer (LUMAT LB 9507, Berthold Technologies), and light emission was recorded in the kinetic mode. The integration time for each reading was 1 s. The interval between readings was 15 s, and total recording time was 4 min. Finally, total cellular protein content of each sample was determined.

Oxygen Consumption Rate Measurement—Intact cell oxygen consumption rate was measured by an Oxygraph system with DW1 Oxygen Electrode (Hansatech Instruments Ltd., Norfolk, UK) as described previously (31). Briefly, RKO cells with CHCM1/CHCHD6 knockdown or scramble knockdown were harvested by tripsinization and centrifugation at 2500 rpm. Approximately 1.5×10^6 cells were resuspended in 300 μl of growth medium for each sample and injected into the polarographic chamber for the intact cell-coupled oxygen consumption rate.

Statistical Analysis—The MTT assay data for the evaluation of cancer cell proliferation and chemosensitivity as well as the cellular ATP production assay and oxygen consumption assay reported in this study were expressed as the mean ± S.E. of three independent experiments. Statistical analysis was performed with one-tailed Student's *t* test. The value of $p < 0.05$ was considered as statistically significant.

RESULTS

CHCM1/CHCHD6 Is a Novel Mitochondrial Protein—We have previously reported the identification and characterization of several novel stress-regulated proteins, including PDRG1, SKNY, DOC45, and RBEL1 (24–25, 32–34). CHCM1/CHCHD6 was also identified in our continuous efforts to identify novel markers of cellular stress response. In particular, we identified CHCM1/CHCHD6 as one of several BBEL1-interacting proteins (BBEL1 is another novel stress-regulated mitochondrial protein identified in our laboratory.[3] Specifically, we performed a standard proteomic screen involving S-tag pull-down and mass spectrometry assays and identified several BBEL1-interacting proteins, including CHCM1/CHCHD6. Sequence corresponding to CHCM1 was found to be annotated in the database as a hypothetical protein (CHCHD6), indicating it to be a novel previously uncharacterized protein. An

[2] The abbreviations used are: MTT, 3-(4,5-dimethylthiazol-2-yl)-2,5-diphenyltetrazolium bromide; CHCH, coiled coil helix-coiled coil helix; OM, outer membrane; IMS, intermembrane space; IM, inner membrane; M, matrix.

[3] J. Shi, Q. He, H. Sun, J. An, K. Lui, J. Montalbano, Y. Liu, Y. Huang, and M. S. Sheikh, manuscript in preparation.

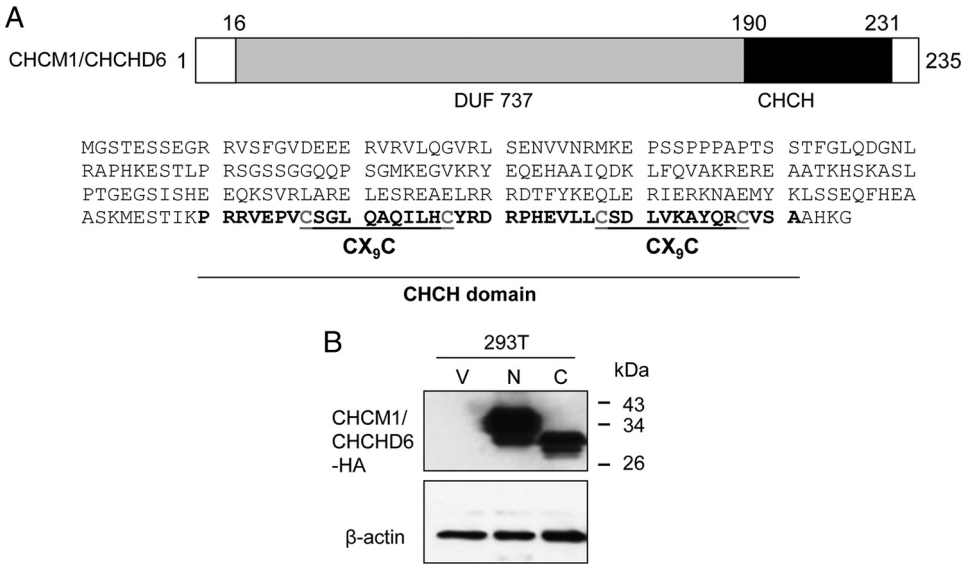

FIGURE 1. *A*, schematic illustration and amino acid sequence of CHCM1/CHCHD6. *DUF*, domain of unknown function. Cysteines in the CX_9CCX_9C motif are *highlighted* in different color. *B*, expression of exogenous CHCM1/CHCHD6 in HEK293T cells. *V*, vector only; *N*, HA-S tagged at the N terminus of CHCM1/CHCHD6; *C*, HA-S tagged at the C terminus of CHCM1/CHCHD6. The N-tagged CHCM1/CHCHD6 migrates more slowly because there are three HA tags.

expressed sequence tag (ATCC) cDNA corresponding to CHCM1/CHCHD6 was sequenced and found to contain an open reading frame composed of 235 amino acids with a predicated molecular mass of 26.5 kDa. CHCM1/CHCHD6 is predicted to have a myristylation site (M*G*STESSEGRRVSFGVDE) at the N-terminal end and a coiled coil helix-coiled coil helix (CHCH) domain at its C-terminal end harboring twin CX_9C structural motifs (Fig. 1*A*). In addition, a DUF737 domain (domain of unknown function) is present at the N terminus (Fig. 1*A*). To ensure that the cDNA corresponding to CHCM1/CHCHD6 encodes a *bona fide* protein of the expected size, we constructed expression vectors in which CHCM1/CHCHD6 cDNA was tagged with HA-S-tag either at the N or C terminus and transfected into HEK293T cells, and its expression was detected by Western blotting. The representative results shown in Fig. 1*B* indicate that the expression vector carrying CHCM1/CHCHD6 expressed CHCM1/CHCHD6 protein in the expected size range, a finding that confirmed that CHCM1/CHCHD6 cDNA encoded a *bona fide* protein. Of note, the N-tagged construct has three HA tags, whereas the C-tagged construct has only one; hence, the CHCM1/CHCHD6 expressed by the former is larger in mass and migrates slower. The C-tagged construct was used in all subsequent experiments.

Next, we sought to investigate the subcellular distribution of CHCM1/CHCHD6, and to that end, we transiently co-transfected HA tag vector alone or expression vector carrying HA-tagged CHCM1/CHCHD6 along with pDsRed2-Mito vector (which expresses red fluorescent protein (RFP) in mitochondria) into MCF7 human breast cancer cells and performed immunostaining using anti-HA antibody. The results shown in Fig. 2*A* indicate that exogenous CHCM1/CHCHD6 displayed localization similar to that noted for mitochondrial RFP (*red*), suggesting CHCM1/CHCHD6 to be a mitochondrial protein (Fig. 2*A*). Cells transfected with HA tag vector alone without CHCM1/CHCHD6 insertion did not display an immunofluorescent pattern resembling that noted for CHCM1/CHCHD6 and thus served as a negative control (data not shown). We also investigated subcellular localization of endogenous CHCM1/CHCHD6 using a polyclonal antibody generated against purified CHCM1/CHCHD6 in our laboratory. Results in Fig. 2*B* indicate that endogenous CHCM1/CHCHD6 displayed mitochondrial localization as well. We also performed cellular fractionations to determine the subcellular distribution of CHCM1/CHCHD6. Results obtained from multiple cell lines shown in Fig. 2*C* indicate that endogenous CHCM1/CHCHD6 was predominantly detected in the mitochondrial fractions. The same blots were also probed to detect Tim23, which is a known mitochondrial protein, and as expected, Tim23 was detected in the mitochondrial fractions (Fig. 2*C*). Using the same approach, we also analyzed subcellular localization of exogenous CHCM1/CHCHD6, and that was also predominantly detected in the mitochondrial fractions (data not shown). Taken together, these results indicate that CHCM1/CHCHD6 is a *bona fide* mitochondrial protein.

Next, we investigated the submitochondrial localization of CHCM1/CHCHD6 and thus performed sucrose gradient centrifugation to enrich purified mitochondria that were subsequently subjected to ultracentrifugations to separate outer membrane (OM), intermembrane space (IMS), inner membrane (IM) and matrix (M) fractions. These fractions were then analyzed by Western blotting, and as is shown (Fig. 3*A*), CHCM1/CHCHD6 was not detected in the OM or IMS fraction but was predominantly present in the IM fraction, and a trace amount was detected also in the M fraction. We also analyzed the submitochondrial distributions of other proteins, such as mitofilin, Smac, HSP60, and VDAC1, that have been reported to localize to different mitochondrial compartments. As shown in Fig. 3*A*, Hsp60, which is known to predominantly reside in the matrix, was also detected in the matrix with trace amounts detected in the OM and IM fractions (*lanes 2* and *4*), a finding consistent with those reported by others that Hsp60 can

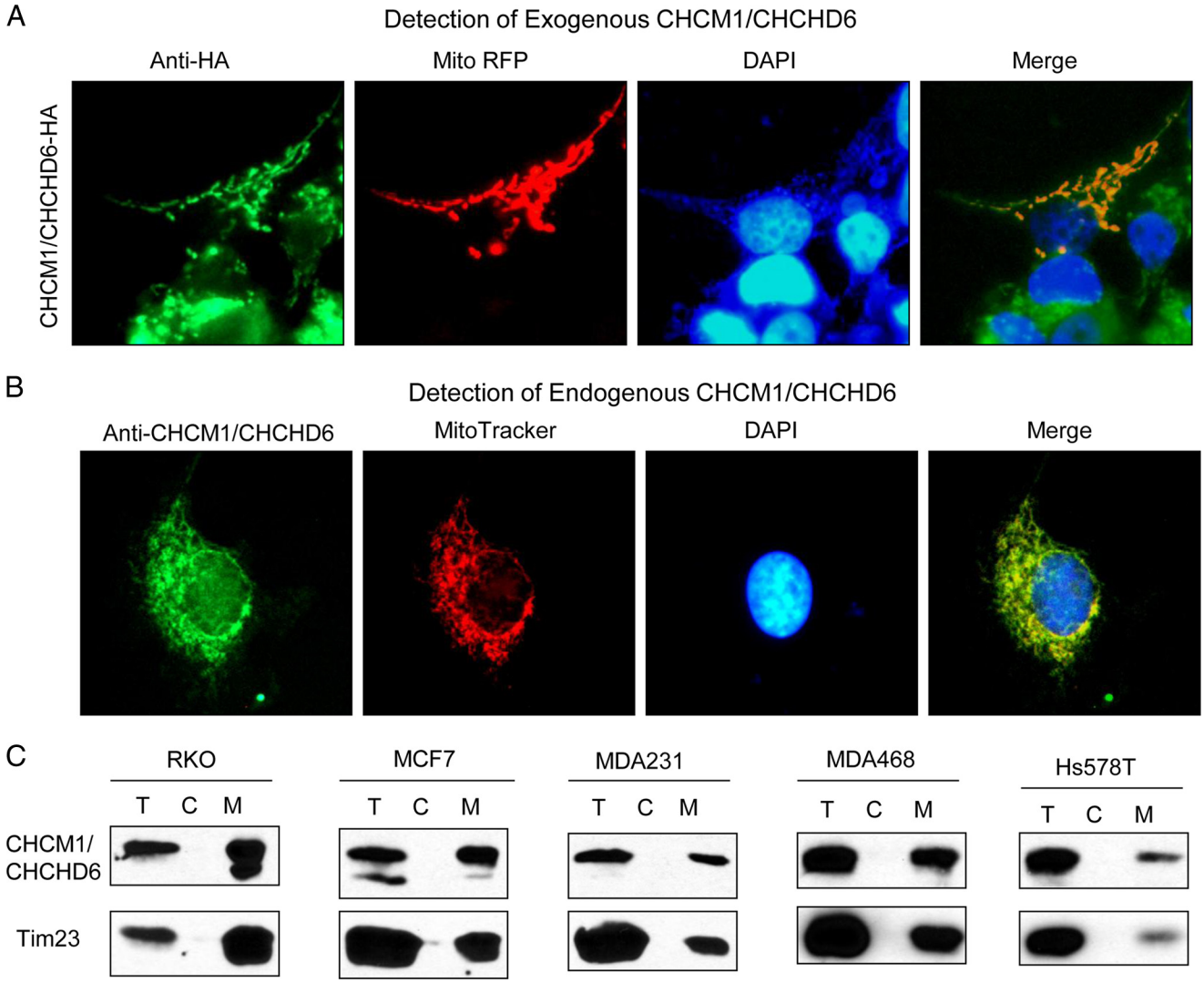

FIGURE 2. **CHCM1/CHCHD6 is a mitochondrial protein.** *A*, representative fluorescent photomicrographs showing the subcellular distribution of exogenous HA-tagged CHCM1/CHCHD6 (*green*) and mitochondria-specific RFP (*red*) in MCF7 cells. *B*, representative fluorescent photomicrographs showing the subcellular distribution of endogenous CHCM1/CHCHD6 (*green*) and MitoTracker staining (*red*) in uacc62 cells. Cells were also stained with DAPI nuclear stain. *C*, subcellular distribution of endogenous CHCM1/CHCHD6 in multiple cell lines. CHCM1/CHCHD6 distribution was determined by the cell fractionation method followed by Western blot analyses. *T*, total cell lysate; *C*, cytosolic fraction; *M*, mitochondrial fraction. Tim23, a mitochondrial protein, was used as a control.

be detected at other sites (35–37). VDAC1 is known to reside in the mitochondrial OM and has been reported to also localize to other subcellular sites, including plasma membrane and the ER (38, 39). As expected, VDAC1 was found in the OM fraction but not in the IMS or M fraction, although it was also detected in the IM fraction (Fig. 3*A*). Smac is an IMS protein, and as expected, it was detected in the IMS fraction (Fig. 3*A*). Smac was also detected in the M fraction but not in the OM or IM fraction (Fig. 3*A*), which may be consistent with recently reported findings that modified Smac localized to the matrix (40). Mitofilin is a known IM protein (41, 42), and, as expected, it was detected predominantly in the IM fraction but not in the OM, IMS, and M fractions (Fig. 3*A*). Thus, the submitochondrial distribution pattern of CHCM1/CHCHD6 is largely similar to that of mitofilin's (Fig. 3*A*, *lane 4*), a finding that indicates that CHCM1/CHCHD6 appears to predominantly localize to the mitochondrial inner membrane.

Computer-based protein structural analyses did not reveal CHCM1/CHCHD6 to contain hydrophobic transmembrane regions. We therefore performed a sodium carbonate extraction assay to determine whether CHCM1/CHCHD6 was an integral membrane protein or a membrane-associated protein. Cellular proteins were first separated into two fractions: (i) a soluble fraction (S_{100}) and (ii) a non-soluble fraction that contained integral membrane proteins as well as membrane-associated proteins. The non-soluble fraction was treated with sodium carbonate to dissociate non-integral membrane-associated proteins. The sodium carbonate-treated lysates were subsequently separated by ultracentrifugation to obtain membrane-associated proteins (supernatants, S_{240}) and the integral membrane proteins (pellets, P_{240}). Western blot analyses were performed to analyze these fractions to detect CHCM1/CHCHD6 as well as markers of membrane-associated (p97) and integral membrane (Tim23) proteins. As shown in Fig. 3*B*,

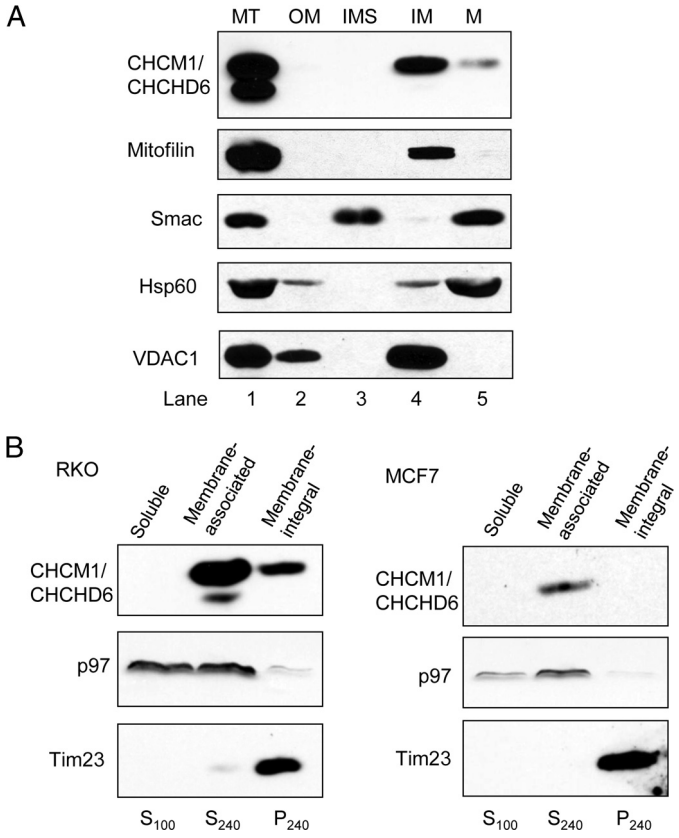

FIGURE 3. *A*, submitochondrial distribution of CHCM1/CHCHD6. Shown are Western blot analyses of submitochondrial fractions. Submitochondrial fractions were prepared using RKO cells as described under "Experimental Procedures." *MT*, total mitochondria fraction. *B*, sodium carbonate extraction-based distribution of CHCM1/CHCHD6. Western blot analyses of samples from sodium carbonate extraction assay in RKO and MCF7 cells. S_{100}, soluble fraction; S_{240}, membrane-associated fraction; P_{240}, integral membrane fraction. p97 serves as a marker of soluble and membrane-associated fractions, and Tim23 serves as a marker of integral membrane fraction.

CHCM1/CHCHD6 was not detected in the soluble (S_{100}) fraction (*lane 1*), but high levels of CHCM1/CHCHD6 were detected in the membrane-associated (S_{240}) fraction (*lane 2*). A small amount of CHCM1 was also detected in the P_{240} fraction (*lane 3*). As expected, p97, a non-integral membrane-associated protein, was detected in the S_{100} and S_{240} fractions (*lanes 1* and *2*). Similarly, Tim23, an integral membrane protein, was predominantly detected in the P_{240} fraction (*lane 3*). Together, these results suggest that CHCM1/CHCHD6 appears to be a membrane-associated protein.

Genotoxic Stress Down-regulates CHCM1/CHCHD6—CHCM1/CHCHD6 is a mitochondrial protein, and certain mitochondrial proteins have been found to affect cell growth and cell death and are also regulated in response to anticancer drug treatment. Therefore, we sought to investigate the effect of anticancer drugs, including etoposide and Adriamycin (doxorubicin), that induce DNA damage (genotoxic stress) using various human cancer cell lines representing different malignancies, and our results indicated that these drugs strongly down-regulated CHCM1/CHCHD6 expression. Fig. 4*A* shows representative Northern blot analyses, indicating that etoposide (*E*) strongly down-regulated CHCM1/CHCHD6 mRNA expression in multiple human cancer cell lines (*C*, untreated controls; *E*, etoposide-treated samples). Kinetics of mRNA down-regulation following Adriamycin treatment (Fig. 4*B*) in RKO human colon cancer cells indicated that CHCM1/CHCHD6 expression was reduced within 12 h, and its effect was maintained until 60 h post-treatment. Using anti-CHCM1/CHCHD6 antibody, we further confirmed that CHCM1/CHCHD6 was down-regulated by these genotoxic drugs also at the protein levels in multiple human cancer cell lines (Fig. 4*C*). Because CHCM1/CHCHD6 is a mitochondrial protein, we also investigated whether it was regulated by mitochondrial respiratory chain inhibitors, including antimycin A and rotenone. Results shown in supplemental Fig. 1, *A* and *B*, indicate that these agents did not appreciably affect the CHCM1/CHCHD6 levels.

CHCM1/CHCHD6 Depletion Reduces Cell Proliferation—To gain insight into the function of CHCM1/CHCHD6, endogenous CHCM1/CHCHD6 was knocked down using a lentiviral shRNA approach. To this end, we utilized a number of lentiviral vectors expressing shRNAs, namely G4, G5, G6, G7, and G8, each targeting a different region of CHCM1/CHCHD6 mRNA. A lentiviral vector with a scrambled sequence as a control was also used. The knockdown efficiency was then tested in various human cancer cell lines. Representative results in Fig. 5*A* show that these constructs effectively knocked down endogenous CHCM1/CHCHD6 at mRNA and protein levels in RKO human colon and MCF-7 breast cancer cells. We next performed an MTT assay to assess the effect of CHCM1/CHCHD6 deficiency in various human cancer cell lines, and as shown in Fig. 5*B*, CHCM1/CHCHD6 knockdown led to significant reduction in cancer cell growth.

CHCM1/CHCHD6 Depletion or Overexpression Alters Chemosensitivity of Human Cancer Cells to Genotoxic Anticancer Drugs—Because CHCM1/CHCHD6 was down-regulated following treatment with genotoxic anticancer drugs, and its depletion affected cancer cell growth, we also investigated the effect of CHCM1/CHCHD6 deficiency on cancer cell growth following treatment with genotoxic anticancer drugs. Results in Fig. 6*A* show that CHCM1/CHCHD6 knockdown further increased etoposide and Adriamycin-mediated chemosensitivity of human cancer cells. We also established RKO human colon cancer cells stably expressing exogenous CHCM1/CHCHD6 and tested their chemosensitivity to etoposide. Results of two independent clones (C3 and C4) are shown in Fig. 6*B*, and as is shown, increased expression of exogenous CHCM1/CHCHD6 in RKO cells resulted in reduced etoposide-mediated chemosensitivity.

CHCM1/CHCHD6 Interacts with Mitofilin, CHCHD3, and DISC1—CHCM1/CHCHD6 exhibits mitochondrial distribution, and interestingly, we noted that mitofilin, a known mitochondrial protein, was also present along with CHCM1/CHCHD6 in our previous proteomic screen when we tried to find BBEL1-interacting proteins. In a study reported by Xie *et al.* (43), mitofilin was found to be present in a complex with multiple proteins, including the hypothetical protein CHCHD6 that corresponds to CHCM1. We therefore sought to investigate mutual interactions between CHCM1/CHCHD6 and mitofilin. First, we performed an S-tag pull-down assay using cell lysates from RKO cells stably expressing exogenous

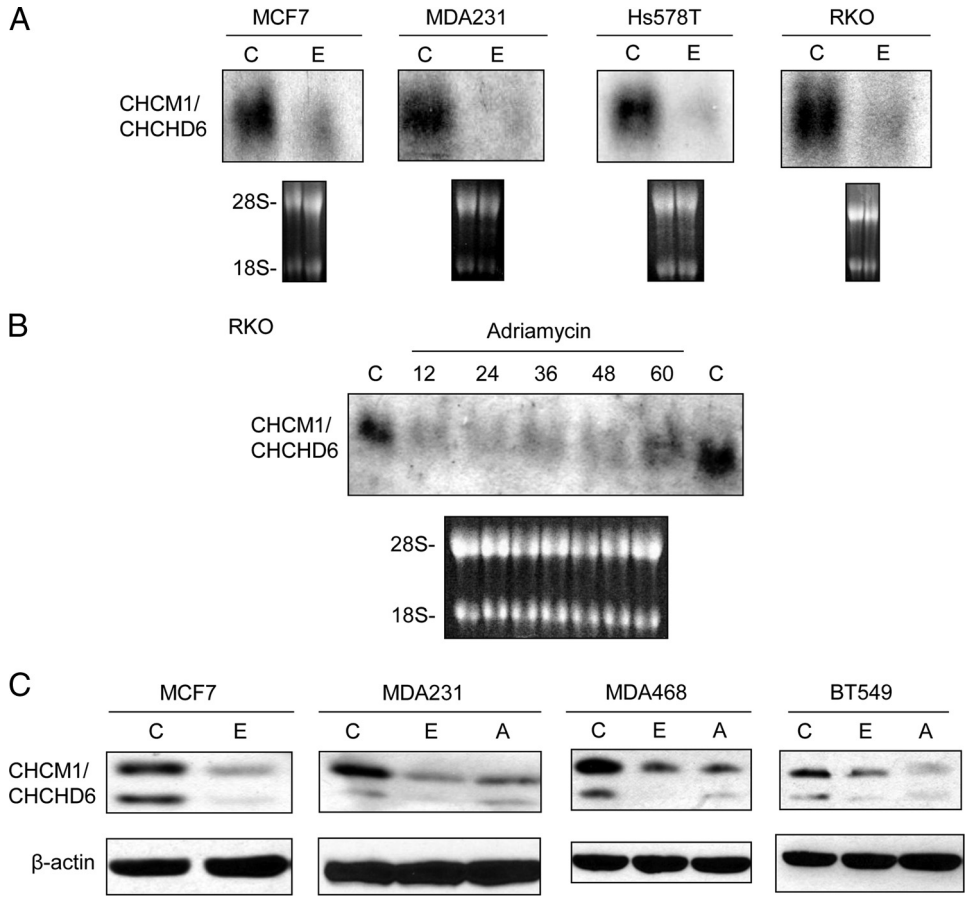

FIGURE 4. **Genotoxic stress down-regulates CHCM1/CHCHD6.** *A*, Northern blot analyses showing the effect of genotoxic etoposide on CHCM1/CHCHD6 mRNA expression in the indicated cell lines. *C*, control; *E*, etoposide, 30 μM for 24 h. *B*, effect of doxorubicin (Adriamycin) on CHCM1/CHCHD6 mRNA levels in RKO cells. Cells were treated with Adriamycin (0.5 μM) for the indicated times in hours. *C*, untreated controls. *C*, Western blot analyses showing DNA damage down-regulation of CHCM1/CHCHD6 protein levels in the indicated cell lines. *C*, control; *E*, etoposide, 30 μM for 24 h; *A*, Adriamycin, 1.0 μM for 24 h.

S-tagged CHCM1/CHCHD6. The results in Fig. 7*A* show that exogenous CHCM1/CHCHD6 strongly interacted with endogenous mitofilin. Next, we performed immunoprecipitation with anti-CHCM1/CHCHD6 antibody and found that endogenous CHCM1/CHCHD6 also strongly interacted with endogenous mitofilin (Fig. 7*B*). These results indicate that CHCM1/CHCHD6 also interacts with mitofilin *in cellulo.*

To date, detailed characterization of mitofilin interactions with two other proteins, including DISC1 (disrupted-in-schizophrenia 1) and CHCHD3, has been reported (13, 14). DISC1 is linked to neurodevelopment and believed to be important for mitofilin stability (13), whereas CHCHD3 is linked to maintaining mitochondrial cristae morphology (14). Therefore, we also investigated whether CHCM1/CHCHD6 interacts with CHCHD3 and/or DISC1. First, we performed S-tag pull-down assay using cell lysates representing crude mitochondrial fractions from RKO cells stably expressing exogenous S-tagged CHCM1/CHCHD6. The results in Fig. 7*C* show that exogenous CHCM1/CHCHD6 interacted with endogenous CHCHD3 and DISC1. Next, we performed immunoprecipitations using anti-CHCM1/CHCHD6 antibodies and found that endogenous CHCM1/CHCHD6 also displayed interactions with endogenous CHCHD3 and DISC1 (Fig. 7*D*). These results indicate that CHCM1/CHCHD6 also interacts with both CHCHD3 and DISC1.

CHCM1/CHCHD6 Is Linked to Maintaining Mitochondria Cristae Morphology—Mitofilin has been reported to reside in the inner membrane of mitochondria and is linked to maintaining mitochondrial cristae morphology (10, 41, 42). Our results confirmed that mitofilin indeed localized to the inner mitochondrial membrane (Fig. 3*A*). Because our results indicated that CHCM1/CHCHD6 also predominantly localized to the inner membrane of mitochondria (Fig. 3*A*) and because it interacted with mitofilin, we sought to investigate whether CHCM1/CHCHD6 was also linked to maintaining mitochondrial cristae morphology. To that end, we knocked down CHCM1/CHCHD6 in three different cells lines, including RKO (human colon cancer), MCF-7 (human breast cancer), and A375 (human melanoma) cells, and analyzed mitochondrial morphology by transmission electron microscopy. Our results indicated that CHCM1/CHCHD6 knockdown in all three cell lines altered mitochondrial morphology. Representative results for RKO and MCF-7 cells are shown in Fig. 8, in which *black arrows* point to normal and *white arrows* indicate abnormal mitochondria. As is shown (Fig. 8, *A* and *B*), the normal mitochondria in scrambled control cells had well defined cristae structures, whereas a larger number of mitochondria in the CHCM1/CHCHD6 knockdown cells (Table 1) displayed clearly altered cristae structures (Fig. 8). Table 1 shows the percentages of mitochondria with abnormal cristae structures in scramble and

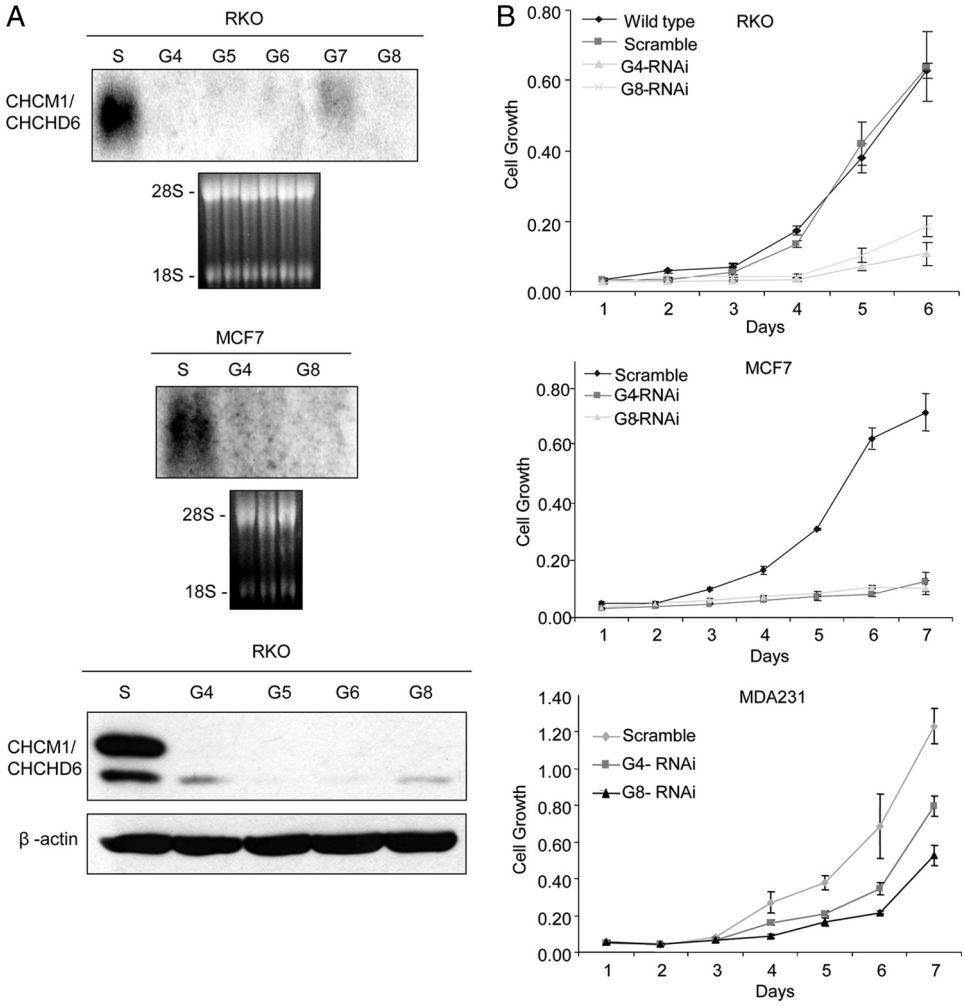

FIGURE 5. **CHCM1/CHCHD6 depletion reduces cell growth.** *A*, Northern and Western blot analyses showing CHCM1/CHCHD6 knockdown in RKO and MCF7 cell lines. *S*, scramble. G4, G5, G6, G7, and G8 are different CHCM1/CHCHD6-shRNA constructs. *B*, MTT assays showing cell growth in scramble or CHCM1/CHCHD6 knockdown cells representing RKO, MCF7, and MDA231 cell lines. G4 and G8 are two different CHCM1/CHCHD6-shRNA constructs. Values represent mean ± S.E. (*error bars*) of triplicate samples.

CHCM1/CHCHD6 knockdown cells. These results therefore indicate that CHCM1/CHCHD6 is also linked to maintaining mitochondrial cristae morphology.

CHCM1/CHCHD6 Directly Interacts with Mitofilin via Its C Terminus—Our preceding results indicate that CHCM1/CHCHD6 strongly interacts with mitofilin (Fig. 7), and just like mitofilin, CHCM1/CHCHD6 knockdown leads to alterations in mitochondrial cristae morphology (Fig. 8). We next undertook studies to (i) investigate whether CHCM1/CHCHD6 directly or indirectly interacts with mitofilin and (ii) identify the region through which CHCM1/CHCHD6 interacts with mitofilin. First, we constructed two separate bacterial expression vectors: one carrying S-tagged CHCM1/CHCHD6 and another with GST-tagged mitofilin. The expression vectors carrying CHCM1/CHCHD6 or mitofilin were independently introduced into *E. coli*, and the expressed proteins were purified. The purified proteins were then used to test their mutual interactions. Results in Fig. 9*A* show that, indeed, the purified CHCM1/CHCHD6 and mitofilin exhibited direct interactions (Fig. 9*A*, *lane 4*). We next generated four deletion variants of CHCM1/CHCHD6 that were lacking 50 or 100 amino acids at their N- or C-terminal ends (Fig. 9*B*). These variants were introduced into bacterial expression vector with S tag at their N-terminal ends and then expressed in *E. coli* and purified. Fig. 9*C* shows Coomassie Blue staining of purified full-length and deletion variants of CHCM1/CHCHD6 (denoted by an *asterisk*). The S-tag pull-down assay was performed using purified CHCM1/CHCHD6 protein variants and gel-purified GST-tagged mitofilin protein, and the resultant precipitants were analyzed by immunoblotting with anti-GST or anti-S-tag antibodies separately. The results (Fig. 9*D*) show that the full-length as well as deletion variants devoid of N-terminal 50 and 100 amino acids exhibited interactions with mitofilin. However, the CHCM1/CHCHD6 deletion variants lacking the C-terminal 50 or 100 amino acids displayed reduced or absent interactions with mitofilin (Fig. 9*D*, *lanes 7* and *8*). These results indicate that the C terminus of CHCM1/CHCHD6, including the CHCH domain appeared to be important for its interaction with mitofilin.

CHCM1/CHCHD6 and Mitofilin Are Coordinately Regulated—Our preceding results indicate that CHCM1/CHCHD6 directly interacts with mitofilin, and just like mitofilin, it is linked to regulating mitochondrial cristae morphology. Next, we analyzed the effect of CHCM1/CHCHD6 knockdown

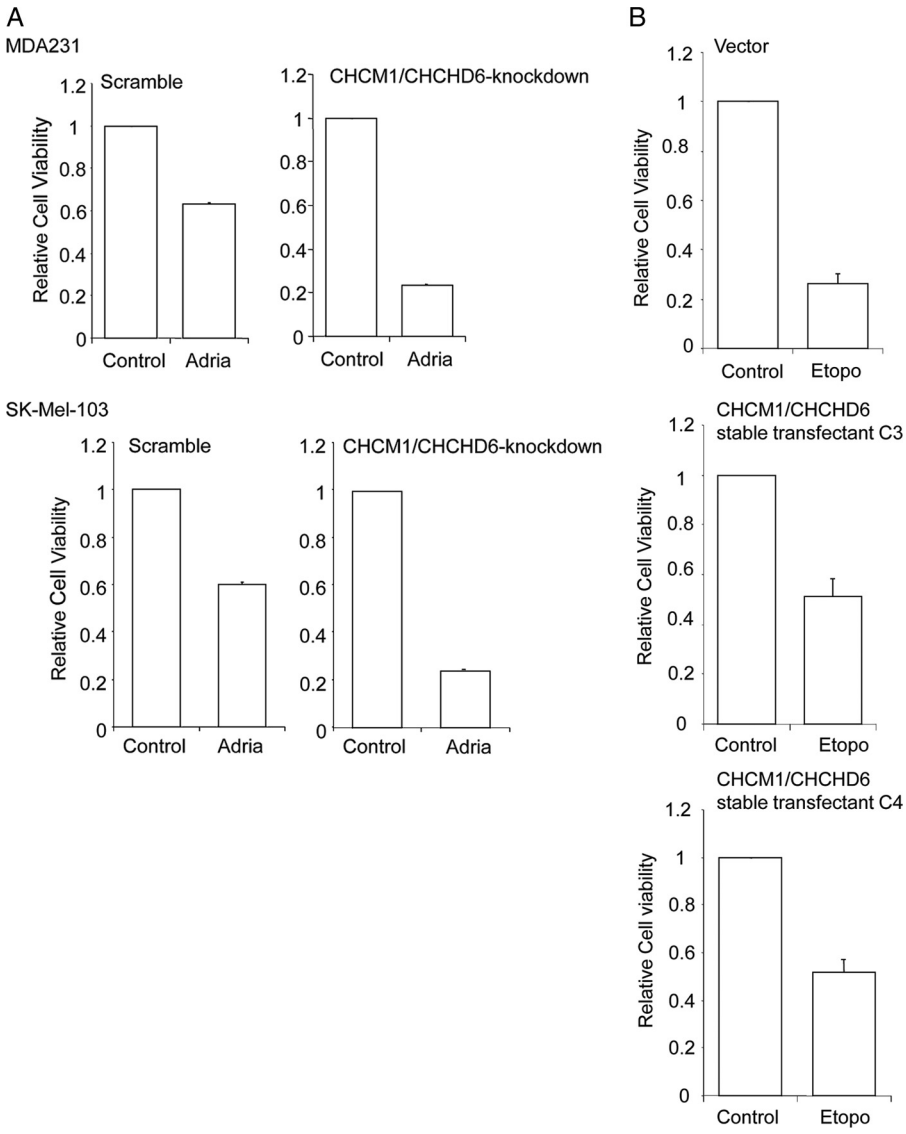

FIGURE 6. **CHCM1/CHCHD6 depletion and overexpression alters chemosensitivity of human cancer cells to genotoxic anticancer drugs.** *A*, CHCM1/CHCHD6 knockdown increases cellular sensitivity to doxorubicin (Adriamycin). MDA231 and SK-Mel-103 cells were untreated or treated with Adriamycin (*Adria*; 3 μM for MDA231 and 1 μM for SK-Mel-103) for 24 h, and cell viability was assessed by an MTT assay. Values represent mean ± S.E. (*error bars*) of triplicate samples. *B*, stable overexpression of CHCM1/CHCHD6 reduces cellular sensitivity to etoposide. RKO cells stably expressing exogenous CHCM1/CHCHD6 or vector-transfected cells were untreated or treated with etoposide (30 μM) for 48 h, and cell viability was determined by an MTT assay. C3 and C4 are two independent CHCM1/CHCHD6 stable transfectants. Values represent mean ± S.E. of triplicate samples.

on mitofilin expression and found that CHCM1/CHCHD6 knockdown resulted in down-regulation of endogenous mitofilin (Fig. 10*A*). It is of note that in some cells, such as the SK-mel103 melanoma cell line, CHCM1/CHCHD6 deficiency reproducibly led to a dramatic decrease in the endogenous mitofilin levels, whereas in some cells, including RKO colon and MCF-7 breast cancer cell lines, the decreases in mitofilin levels were less dramatic or minimal varying from experiment to experiment. We also performed the reverse experiments and investigated the effect of mitofilin deficiency on CHCM1/CHCHD6 levels and noted that mitofilin deficiency also led to a decrease in CHCM1/CHCHD6 levels (Fig. 10*B*). The effect of increased expression of CHCM1/CHCD6 was also analyzed using RKO colon cancer cells stably expressing exogenous CHCM1/CHCHD6, and as shown in Fig. 10*C*, overexpression of exogenous CHCM1/CHCHD6 increased expression level of endogenous mitofilin. Together, these results indicate that the expression levels of both proteins are coordinately regulated, and a cross-talk appears to exist between these two proteins modulating their regulation and function.

CHCM1/CHCHD6 Deficiency Induces Mitochondrial Dysfunction—Because CHCM1/CHCHD6 knockdown affected mitochondrial cristae morphology, we also investigated the effect of CHCM1/CHCHD6 deficiency on mitochondrial function. To that end, we performed a luciferase-based assay to measure cellular and mitochondrial ATP synthesis in CHCM1/CHCHD6-proficient and -deficient cells. Our results (Fig. 11*A*) indicated that CHCM1/CHCHD6 deficiency clearly affected total as well as mitochondrial ATP synthesis. We also compared oxygen consumption rate in CHCM1/CHCHD6-proficient and -deficient cells, and as shown in Fig. 11*B*, knockdown of CHCM1/CHCHD6 led to a clear decrease in oxygen con-

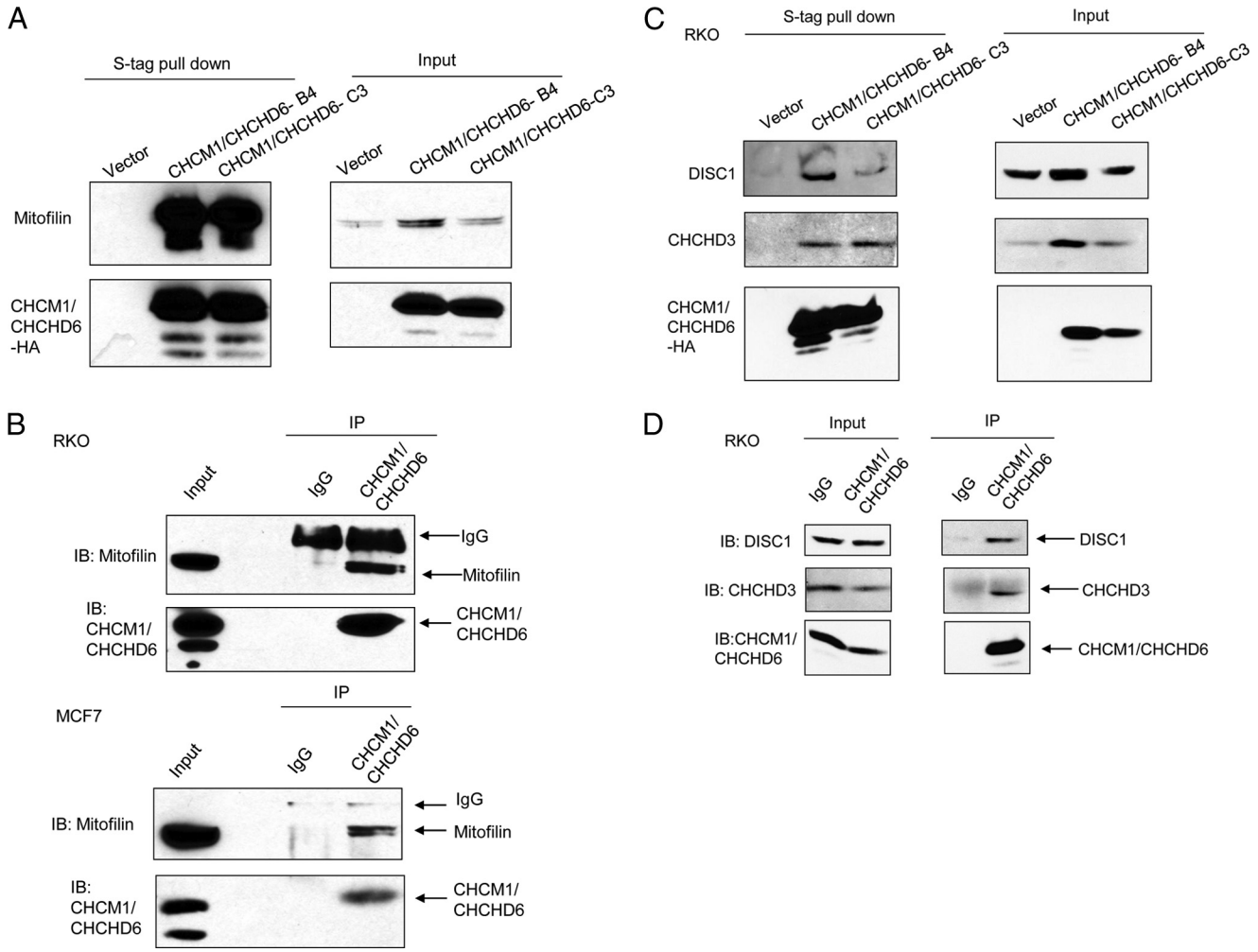

FIGURE 7. **CHCM1/CHCHD6 interacts with mitofilin, DISC1, and CHCHD3.** *A*, exogenous CHCM1/CHCHD6 interacts with endogenous mitofilin. S-tag pull-down analyses were performed on vector-transfected or CHCM1/CHCHD6-transfected RKO cells. CHCM1/CHCHD6-B4 and CHCM1/CHCHD6-C3 are independent stable transfectants that express exogenous HA-S-tagged CHCM1/CHCHD6. S-tag pull-down was done with S-tag-agarose beads, and Western blot analyses were done with the indicated antibodies. *B*, endogenous CHCM1/CHCHD6 interacts with endogenous mitofilin. RKO and MCF7 cell lysates were used for CHCM1/CHCHD6 immunoprecipitation (*IP*) by anti-CHCM1/CHCHD6 antibody, and Western blot analyses (*IB*) were done with the indicated antibodies. *NS*, nonspecific binding. *C*, exogenous CHCM1/CHCHD6 interacts with endogenous DISC1 and CHCHD3. S-tag pull-down analyses were performed on crude mitochondria lysate from vector-transfected or CHCM1/CHCHD6-transfected RKO cells. CHCM1/CHCHD6-B4 and CHCM1/CHCHD6-C3 are independent stable transfectants that express exogenous HA-S-tagged CHCM1/CHCHD6. S-tag pull-down was done with S-tag-agarose beads, and Western blot analysis was done with the indicated antibodies. *D*, endogenous CHCM1/CHCHD6 interacts with endogenous DISC1 and CHCHD3. Crude mitochondria lysate from RKO cell was used for CHCM1/CHCHD6 immunoprecipitation by anti-CHCM1/CHCHD6 antibody, and Western blot analyses were done with the indicated antibodies.

sumption rate. These results thus indicate that CHCM1/CHCHD6 knockdown also affects mitochondrial function.

DISCUSSION

In the present study, we report the identification and characterization of CHCM1/CHCHD6, a novel mitochondrial protein that predominantly localizes to the mitochondrial inner membrane. We have also found that the depletion of endogenous CHCM1/CHCHD6 alters mitochondrial cristae morphology. In CHCM1/CHCHD6-deficient cells, the affected mitochondrial cristae appear to be hollow with a loss of structural definition and reduction in electron-dense matrix. Published evidence indicates that the depletion of mitofilin, another mitochondrial inner membrane protein, also alters mitochondrial cristae morphology (10, 41, 42). Interestingly, CHCM1/CHCHD6 strongly and directly interacts with mitofilin. CHCM1/CHCHD6 appears to interact with mitofilin through its C-terminal end, and the C-terminal 50 amino acids harboring the CHCH domain appear to be critical for these interactions. Furthermore, CHCM1/CHCHD6 and mitofilin are coordinately regulated because mitofilin levels are reduced in CHCM1/CHCHD6-deficient cells, and CHCM1/CHCHD6 levels are decreased in mitofilin knockdown cells. Thus, CHCM1/CHCHD6 and mitofilin appear to be critical partners in maintaining the structural integrity of the mitochondrial cristae.

The molecular basis for the coordinate regulation between CHCM1/CHCHD6 and mitofilin remains to be fully elucidated. Mitofilin is believed to exist in a larger protein complex; it is possible that both CHCM1/CHCHD6 and mitofilin reside in the same multiprotein complex, and depletion of either one disrupts the complex formation. A previously published ultra-

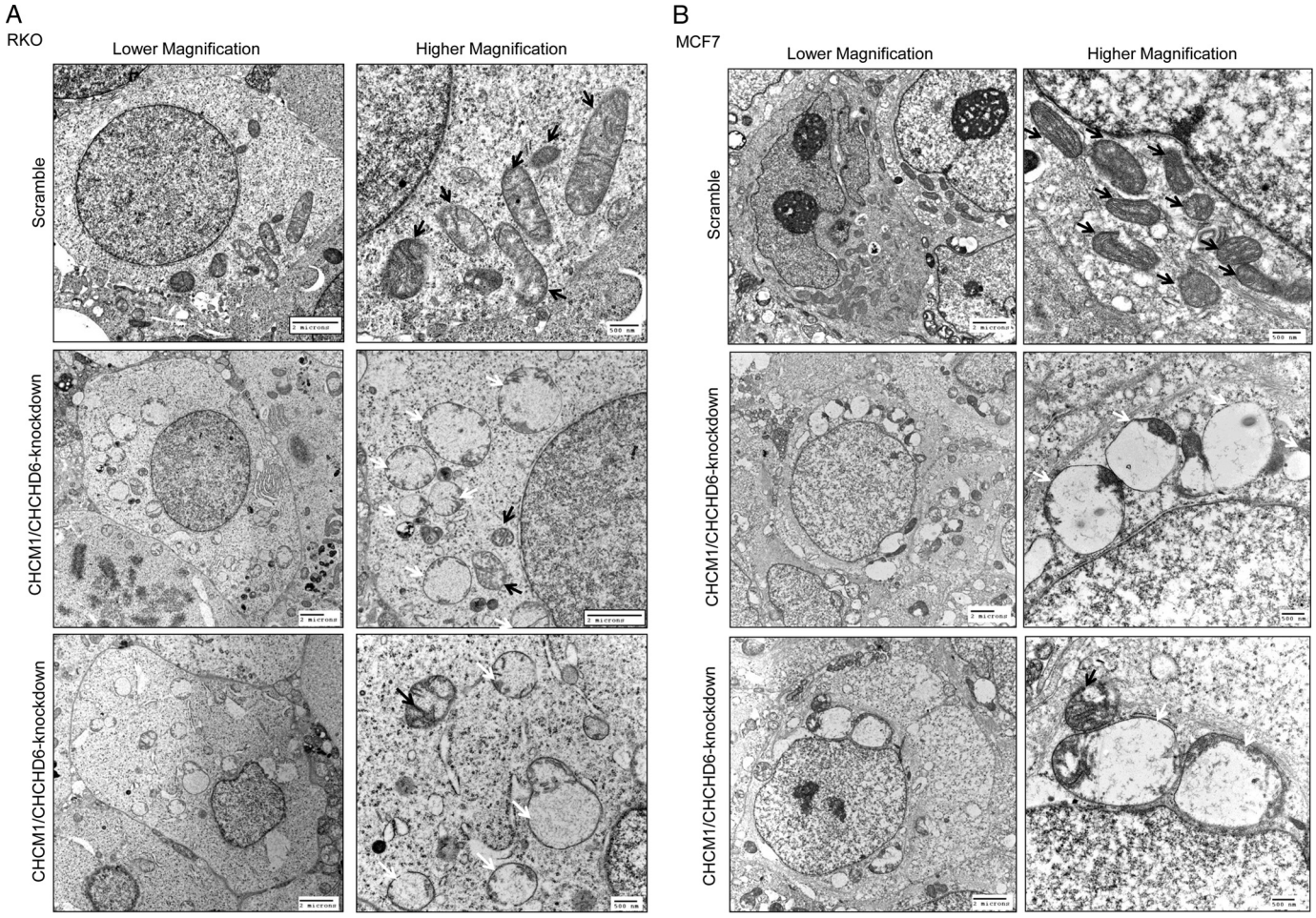

FIGURE 8. **CHCM1/CHCHD6 knockdown affects mitochondria cristae morphology.** Shown are EM analyses of scramble and CHCM1/CHCHD6 knockdown RKO (*A*) and MCF7 cells (*B*). *Black arrows*, normal mitochondria. *White arrows*, mitochondria with abnormal cristae structures.

TABLE 1

Percentage of abnormal mitochondria devoid or nearly devoid of cristae structures in scramble and CHCM1/CHCHD6 knockdown cells

Samples	Abnormal mitochondria	
	Experiment 1	Experiment 2
RKO-scramble	5.5% (5/91)	2.8% (3/106)
RKO-CHCM1/CHCHD6 (KD-G8)	55.6% (109/196)	70.5% (74/105)
RKO-CHCM1/CHCHD6 (KD-G4)	17.8% (30/169)	
MCF7-scramble	6.25% (11/176)	
MCF7-CHCM1/CHCHD6 (KD-G8)	65.2% (723/1109)	
MCF7-CHCM1/CHCHD6 (KD-G4)	58.3% (833/1428)	

structural analysis of mitochondria from mitofilin-deficient cells indicates that the mitochondrial inner membrane exhibits "onion-like concentric spherical" structures as well as layers of "tightly packed concentric-membranous sheets" (10). By contrast, CHCM1/CHCHD6 knockdown more severely affects mitochondrial cristae structures because most of the CHCM1/CHCHD6-deficient mitochondria are devoid of well defined cristae structures. For example, in the CHCM1/CHCHD6-deficient cells, the affected mitochondrial cristae appear to be hollow, with loss of structural definitions and reduction in electron-dense matrix. Thus, the mitochondrial ultrastructure alterations due to loss of mitofilin are morphologically distinct from those noted due to CHCM1/CHCHD6 depletion. It is possible that CHCM1/CHCHD6, in addition to its interactions with mitofilin, may exhibit cross-talk with other mitochondrial proteins to regulate structural integrity of mitochondrial cristae.

Mitofilin is believed to exhibit homotypic interactions in addition to its interactions with other mitochondrial proteins (10, 43). To date, mitofilin interactions with two other proteins, including DISC1 (disrupted-in-schizophrenia 1) and CHCHD3, have been investigated in detail (13, 14). Alterations in DISC1 structure/function are linked to pathogenesis of schizophrenia that is believed to be a neuronal disorder (13). A portion of DISC1 has been reported to reside in mitochondria and interacts with mitofilin. DISC1 deficiency is reported to be associated with mitochondrial dysfunction, mitofilin ubiquitination, and alterations in cristae morphology (13). Interestingly, the morphological features of cristae structures due to DISC1 depletion are similar to those noted due to mitofilin deficiency. Therefore, alterations in the function of DISC1 and mitofilin are thought to be linked to pathogenesis of schizophrenia (13). In our study, we have found that CHCM1/CHCHD6 also interacts with DISC1. The functional basis of CHCM1/CHCHD6 interaction with DISC1 remains to be elucidated and will be the focus of our future investigations.

A more recent study has reported the identification and characterization of CHCHD3 as a novel mitochondrial protein (14). CHCHD3 localizes to the inner mitochondrial membrane and also interacts with mitofilin. Interestingly, we have found

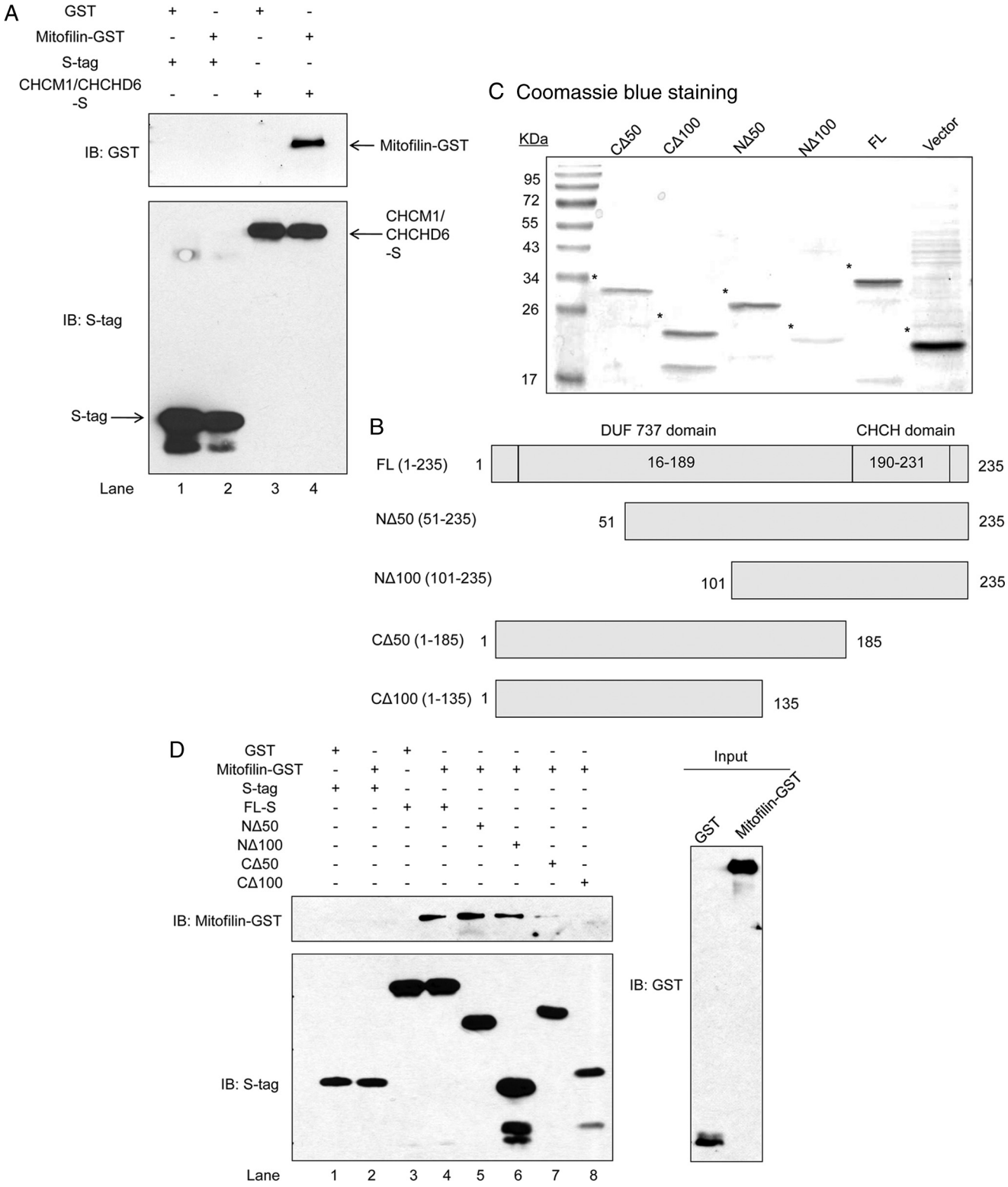

FIGURE 9. **CHCM1/CHCHD6 directly interacts with mitofilin via its C-terminal end.** *A*, direct interaction between CHCM1/CHCHD6 and mitofilin. Purified S-tagged full-length CHCM1/CHCHD6 was incubated with gel-purified mitofilin-GST or GST proteins, and S-tag pull-down assays were performed. The pull-down protein products were analyzed by Western blot (*IB*) using anti-S or anti-GST antibodies. *B*, schematic illustration of the full-length and deletion variants of CHCM1/CHCHD6 protein. *C*, Coomassie Blue staining of recombinant full-length and deletion variants of CHCM1/CHCHD6 from bacteria lysate. S-tag pull-down of recombinant full-length and deletion variants of CHCM1/CHCHD6 was performed on bacteria lysates. The CHCM1/CHCHD6 protein products are indicated by *asterisks*. *D*, mapping of CHCM1/CHCHD6 and mitofilin interaction region on CHCM1/CHCHD6. *Left*, purified S-tagged full-length CHCM1/CHCHD6 and deletion variants were incubated with gel-purified mitofilin-GST or GST protein. Then S-tag pull-downs were performed. The pull-down protein products were analyzed by Western blot using anti-S and anti-GST antibodies. *Right*, Western blot analysis of ~1% input of purified GST and mitofilin-GST proteins.

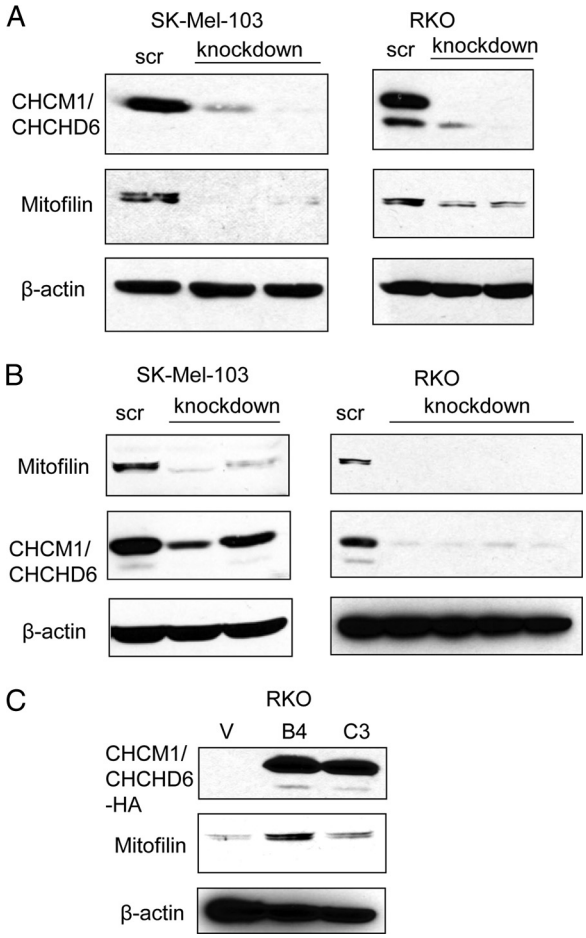

FIGURE 10. **CHCM1/CHCHD6 and mitofilin are coordinately regulated.** *A*, Western blot analysis of mitofilin levels in scramble (*scr*) or CHCM1/CHCHD6 knockdown SK-Mel-103 and RKO cells. *B*, Western blot analysis of CHCM1/CHCHD6 levels in scramble or mitofilin knockdown SK-Mel-103 and RKO cells. Western blot analyses were performed using anti-CHCM1/CHCHD6 or anti-mitofilin antibodies. *C*, Western blot analysis of mitofilin levels in two independent stable transfectants (B4 and C3) that express exogenous HA-S-tagged CHCM1/CHCHD6. Respective blots were also probed with anti-*β*-actin antibody as loading control. Results in *C* are the same as shown also for input in Fig. 7*A*.

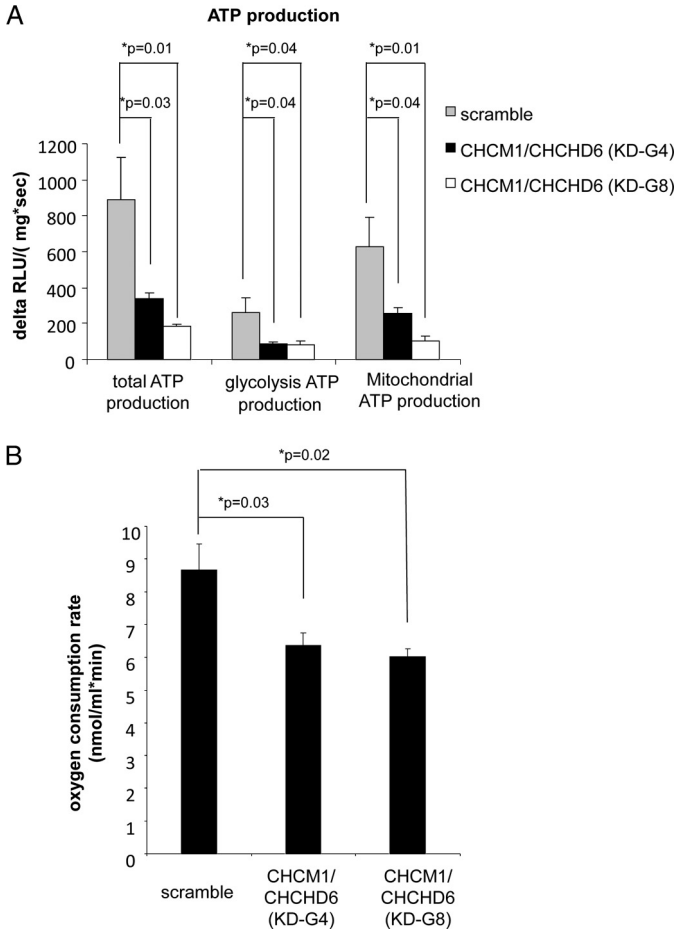

FIGURE 11. **CHCM1/CHCHD6 deficiency induces mitochondrial dysfunction.** *A*, CHCM1/CHCHD6 knockdown affects cellular ATP production. ATP levels in scrambled and CHCM1/CHCHD6 knocked down cells were determined as described under "Experimental Procedures." G4 and G8 are two independent knockdown cells achieved via two different CHCM1/CHCHD6-shRNA constructs. Values represent average ± S.E. (*error bars*) of four independent experiments. *, $p < 0.05$. *B*, CHCM1/CHCHD6 knockdown affects oxygen consumption rate. Oxygen consumption rates in scrambled and CHCM1/CHCHD6 knocked down cells were determined as described under "Experimental Procedures." G4 and G8 are two independent knockdown cells achieved via two different CHCM1/CHCHD6-shRNA constructs. Values represent average ± S.E. of three independent experiments. *, $p < 0.05$.

that CHCM1/CHCHD6 also interacts with CHCHD3. CHCHD3 knockdown also leads to alterations in mitochondrial cristae morphology. Interestingly, just like CHCM1/CHCHD6, CHCHD3 also harbors a CHCH domain at its C-terminal end and exhibits 36% amino acid identity with CHCM1/CHCHD6. Furthermore, knockdown of CHCHD3 results in reduced cell proliferation, and the morphological abnormalities of mitochondrial cristae due to CHCHD3 knockdown appear to be similar to those noted in CHCM1/CHCHD6-deficient cells. However, CHCHD3 knockdown is reported to minimally affect the total cellular ATP levels, whereas CHCM1/CHCHD6 knockdown profoundly affects the total cellular and mitochondrial ATP levels. Thus, CHCM1/CHCHD6 and CHCHD3 are two novel mitochondrial proteins that appear to exhibit similar and distinct characteristics. Furthermore, we have found that CHCM1/CHCHD6 deficiency is not associated with down-regulation of endogenous CHCHD3 (supplemental Fig. 2) a finding that suggests that mitochondrial dysfunction due to CHCM1/CHCHD6 deficiency does not appear to secondarily occur due to down-regulation of endogenous CHCHD3.

In addition to aforementioned proteins, OPA1 and MICS1 are two additional inner mitochondrial membrane proteins that are also linked to maintaining the integrity of cristae morphology (6, 7–9, 11). In the case of OPA1 depletion, the mitochondria display "wider" (7) cristae structure (7–9), whereas MICS1 deficiency leads to "mild fragmentation, lump-like structures, and short curved tubules" (11) in mitochondrial cristae. Clearly, the morphologic features of mitochondrial cristae due to OPA1 or MICS1 deficiency are different from those noted due to mitofilin, DISC1, CHCHD3, or CHCM1/CHCHD6 depletion. OPA1 or MICS1 has not been reported to interact with mitofilin; it will be interesting to investigate CHCM1/CHCHD6 interactions with OPA1 and/or MICS1 and their effects on its function.

It is evident that CHCM1/CHCHD6 appears to be needed for the structural integrity of mitochondrial cristae because mito-

chondrial ultrastructure alterations due to CHCM1/CHCHD6 deficiency are more severe than those noted due to the loss of mitofilin and other mitochondrial proteins. Indeed, CHCM1/CHCHD6 depletion is associated with down-regulation of mitofilin, and such an effect is more dramatic in some cells, whereas in some cells, mitofilin down-regulation following CHCM1/CHCHD6 is not very robust. It is possible that CHCM1/CHCHD6 depletion-mediated alterations in mitochondrial cristae morphology could partly result due to concomitant down-regulation of mitofilin. We have also found that CHCM1/CHCHD6 deficiency does not lead to down-regulation of endogenous CHCHD3 (supplemental Fig. 2). These findings would therefore indicate that CHCM1/CHCHD6 depletion-mediated alterations in mitochondrial cristae morphology do not appear to occur through deficiency in CHCHD3 levels and thus point to unique functional characteristic of CHCM1/CHCHD6 in maintaining mitochondrial cristae morphology. It is conceivable that CHCM1/CHCHD6 via its interactions with mitofilin, CHCHD3, and DISC1 and/or with some of the other mitochondrial proteins may exert a tight control over structural integrity and biogenesis of mitochondrial cristae. CHCM1/CHCHD6 deficiency could lead to loss of its interactions with other proteins, and that might severely affect the dynamics of these processes. It is possible that CHCM1/CHCHD6, directly or indirectly, also regulates and fine tunes the processing of other mitochondrial events as its expression is down-regulated, at both mRNA and protein levels, by genotoxic (DNA damage-inducing) anticancer drugs in human cancer cells. CHCM1/CHCHD6 knockdown affects cancer cell growth and enhances chemosensitivity to anticancer drugs. By contrast, increased expression of exogenous CHCM1/CHCHD6 desensitizes cancer cells to these agents. These findings, therefore, also highlight the potential of CHCM1/CHCHD6 as a possible target for cancer therapeutics.

Acknowledgments—We thank Masako Nakatsugawa (Department of Cell and Developmental Biology), Dr. Joyce Qi (Electron Microscopy Laboratory), and Dr. Stephan Wilkens (Department of Biochemistry) at SUNY Upstate Medical University for help with EM samples. We thank Dr. David M. Markovitz (Department of Internal Medicine, University of Michigan Medical Center) for providing SK-Mel-103 and UACC-62 melanoma cell lines (originally from Dr. Maria S. Soengas, Melanoma Laboratory, Spanish National Cancer Research Center) and Dr. Nihal Ahmad (University of Wisconsin, Madison, WI) for providing the A375 melanoma cell line. We thank Dr. Carmen A. Mannella (New York State Department of Health-Wadsworth Center, Albany, NY) for advice on submitochondrial localization experiments. We also thank Dr. Andras Perl and Zachary Oaks (SUNY Upstate Medical University) for help with the oxygen consumption assay.

REFERENCES

1. Czarnecka, A. M., Marino Gammazza, A., Di Felice, V., Zummo, G., and Cappello, F. (2007) Cancer as a "Mitochondriopathy." *J. Cancer Mol.* **3,** 71–79
2. Kirkinezos, I. G., and Moraes, C. T. (2001) Reactive oxygen species and mitochondrial diseases. *Semin. Cell Dev. Biol.* **12,** 449–457
3. Toyokuni, S., Okamoto, K., Yodoi, J., and Hiai, H. (1995) Persistent oxidative stress in cancer. *FEBS Lett.* **358,** 1–3
4. Warburg, O. (1956) On the origin of cancer cells. *Science* **123,** 309–314
5. Carew, J. S., and Huang, P. (2002) Mitochondrial defects in cancer. *Mol. Cancer.* **1,** 9
6. Zick, M., Rabl, R., and Reichert, A. S. (2009) Cristae formation-linking ultrastructure and function of mitochondria. *Biochim. Biophys. Acta* **1793,** 5–19
7. Frezza, C., Cipolat, S., Martins de Brito, O., Micaroni, M., Beznoussenko, G. V., Rudka, T., Bartoli, D., Polishuck, R. S., Danial, N. N., De Strooper, B., and Scorrano, L. (2006) OPA1 controls apoptotic cristae remodeling independently from mitochondrial fusion. *Cell* **126,** 177–189
8. Cipolat, S., Rudka, T., Hartmann, D., Costa, V., Serneels, L., Craessaerts, K., Metzger, K., Frezza, C., Annaert, W., D'Adamio, L., Derks, C., Dejaegere, T., Pellegrini, L., D'Hooge, R., Scorrano, L., and De Strooper, B. (2006) Mitochondrial rhomboid PARL regulates cytochrome *c* release during apoptosis via OPA1-dependent cristae remodeling. *Cell* **126,** 163–175
9. Gottlieb, E. (2006) OPA1 and PARL keep a lid on apoptosis. *Cell* **126,** 27–29
10. John, G. B., Shang, Y., Li, L., Renken, C., Mannella, C. A., Selker, J. M., Rangell, L., Bennett, M. J., and Zha, J. (2005) The mitochondrial inner membrane protein mitofilin controls cristae morphology. *Mol. Biol. Cell* **16,** 1543–1554
11. Oka, T., Sayano, T., Tamai, S., Yokota, S., Kato, H., Fujii, G., and Mihara, K. (2008) Identification of a novel protein MICS1 that is involved in maintenance of mitochondrial morphology and apoptotic release of cytochrome *c*. *Mol. Biol. Cell* **19,** 2597–2608
12. Velours, J., Dautant, A., Salin, B., Sagot, I., and Brèthes, D. (2009) Mitochondrial F_1F_0-ATP synthase and organellar internal architecture. *Int. J. Biochem. Cell Biol.* **41,** 1783–1789
13. Park, Y. U., Jeong, J., Lee, H., Mun, J. Y., Kim, J. H., Lee, J. S., Nguyen, M. D., Han, S. S., Suh, P. G., and Park, S. K. (2010) Disrupted-in-schizophrenia 1 (DISC1) plays essential roles in mitochondria in collaboration with mitofilin. *Proc. Natl. Acad. Sci. U.S.A.* **107,** 17785–17790
14. Darshi, M., Mendiola, V. L., Mackey, M. R., Murphy, A. N., Koller, A., Perkins, G. A., Ellisman, M. H., and Taylor, S. S. (2011) ChChd3, an inner mitochondrial membrane protein, is essential for maintaining crista integrity and mitochondrial function. *J. Biol. Chem.* **286,** 2918–2932
15. Rong, R., Jin, W., Zhang, J., Sheikh, M. S., and Huang, Y. (2004) Tumor suppressor RASSF1A is a microtubule-binding protein that stabilizes microtubules and induces G_2/M arrest. *Oncogene* **23,** 8216–8230
16. Powell, M. J., Casimiro, M. C., Cordon-Cardo, C., He, X., Yeow, W. S., Wang, C., McCue, P. A., McBurney, M. W., and Pestell, R. G. (2011) Disruption of a Sirt1-dependent autophagy checkpoint in the prostate results in prostatic intraepithelial neoplasia lesion formation. *Cancer Res.* **71,** 964–975
17. Yang, J., Liu, X., Bhalla, K., Kim, C. N., Ibrado, A. M., Cai, J., Peng, T. I., Jones, D. P., and Wang, X. (1997) Prevention of apoptosis by Bcl-2. Release of cytochrome *c* from mitochondria blocked. *Science* **275,** 1129–1132
18. Magalhães, P. J., Andreu, A. L., and Schon, E. A. (1998) Evidence for the presence of 5S rRNA in mammalian mitochondria. *Mol. Biol. Cell* **9,** 2375–2382
19. Murthy, M. S., and Pande, S. V. (1987) Malonyl-CoA binding site and the overt carnitine palmitoyltransferase activity reside on the opposite sides of the outer mitochondrial membrane. *Proc. Natl. Acad. Sci. U.S.A.* **84,** 378–382
20. Prasannan, P., and Appling, D. R. (2009) Human mitochondrial C1-tetrahydrofolate synthase. Submitochondrial localization of the full-length enzyme and characterization of a short isoform. *Arch. Biochem. Biophys.* **481,** 86–93
21. Fujiki, Y., Hubbard, A. L., Fowler, S., and Lazarow, P. B. (1982) Isolation of intracellular membranes by means of sodium carbonate treatment. Application to endoplasmic reticulum. *J. Cell Biol.* **93,** 97–102
22. Lui, H. M., Chen, J., Wang, L., and Naumovski, L. (2003) ARMER, apoptotic regulator in the membrane of the endoplasmic reticulum, a novel inhibitor of apoptosis. *Mol. Cancer Res.* **1,** 508–518
23. Luo, X., He, Q., Huang, Y., and Sheikh, M. S. (2005) Transcriptional up-regulation of PUMA modulates endoplasmic reticulum calcium pool depletion-induced apoptosis via Bax activation. *Cell Death Differ.* **12,**

1310–1318
24. Luo, X., Huang, Y., and Sheikh, M. S. (2003) Cloning and characterization of a novel gene, PDRG, that is differentially regulated by p53 and ultraviolet radiation. *Oncogene* **22,** 7247–7257
25. Montalbano, J., Jin, W., Sheikh, M. S., and Huang, Y. (2007) RBEL1 is a novel gene that encodes a nucleocytoplasmic Ras superfamily GTP-binding protein and is overexpressed in breast cancer. *J. Biol. Chem.* **282,** 37640–37649
26. He, Q., Shi, J., Jones, S., An, J., Liu, Y., Huang, Y., and Sheikh, M. S. (2009) Smac deficiency affects endoplasmic reticulum stress-induced apoptosis in human colon cancer cells. *Mol. Cell. Pharmacol.* **1,** 23–28
27. Corcoran, C. A., Montalbano, J., Sun, H., He, Q., Huang, Y., and Sheikh, M. S. (2009) Identification and characterization of two novel isoforms of Pirh2 ubiquitin ligase that negatively regulate p53 independent of RING finger domains. *J. Biol. Chem.* **284,** 21955–21970
28. Moffat, J., Grueneberg, D. A., Yang, X., Kim, S. Y., Kloepfer, A. M., Hinkle, G., Piqani, B., Eisenhaure, T. M., Luo, B., Grenier, J. K., Carpenter, A. E., Foo, S. Y., Stewart, S. A., Stockwell, B. R., Hacohen, N., Hahn, W. C., Lander, E. S., Sabatini, D. M., and Root, D. E. (2006) A lentiviral RNAi library for human and mouse genes applied to an arrayed viral high content screen. *Cell* **124,** 1283–1298
29. Ito, S., and Karnovsky, M. J. (1968) Formaldehyde/glutaraldehyde fixatives containing trinitro compounds. *J. Cell Biol.* **39,** 168a–169a
30. Vives-Bauza, C., Yang, L., and Manfredi, G. (2007) Assay of mitochondrial ATP synthesis in animal cells and tissues. *Methods Cell Biol.* **80,** 155–171
31. Barrientos, A. (2002) *In vivo* and *in organello* assessment of OXPHOS activities. *Methods.* **26,** 307–316
32. Corcoran, C. A., He, Q., Ponnusamy, S., Ogretmen, B., Huang, Y., and Sheikh, M. S. (2008) Neutral sphingomyelinase-3 is a DNA damage and nongenotoxic stress-regulated gene that is deregulated in human malignancies. *Mol. Cancer Res.* **6,** 795–807
33. Sun, H., Luo, X., Montalbano, J., Jin, W., Shi, J., Sheikh, M. S., and Huang, Y. (2010) DOC45, a novel DNA damage-regulated nucleocytoplasmic ATPase that is overexpressed in multiple human malignancies. *Mol. Cancer Res.* **8,** 57–66
34. Montalbano, J., Lui, K., Sheikh, M. S., and Huang, Y. (2009) Identification and characterization of RBEL1 subfamily of GTPases in the Ras superfamily involved in cell growth regulation. *J. Biol. Chem.* **284,** 18129–18142
35. Ghosh, J. C., Siegelin, M. D., Dohi, T., and Altieri, D. C. (2010) Heat shock protein 60 regulation of the mitochondrial permeability transition pore in tumor cells. *Cancer Res.* **70,** 8988–8993
36. Goh, Y. C., Yap, C. T., Huang, B. H., Cronshaw, A. D., Leung, B. P., Lai, P. B., Hart, S. P., Dransfield, I., and Ross, J. A. (2011) Heat-shock protein 60 translocates to the surface of apoptotic cells and differentiated megakaryocytes and stimulates phagocytosis. *Cell Mol. Life Sci.* **68,** 1581–1592
37. Merendino, A. M., Bucchieri, F., Campanella, C., Marcianò, V., Ribbene, A., David, S., Zummo, G., Burgio, G., Corona, D. F., Conway de Macario, E., Macario, A. J., and Cappello, F. (2010) Hsp60 is actively secreted by human tumor cells. *PLoS One* **5,** e9247
38. Shoshan-Barmatz, V., Zalk, R., Gincel, D., and Vardi, N. (2004) Subcellular localization of VDAC in mitochondria and ER in the cerebellum. *Biochim. Biophys. Acta* **1657,** 105–114
39. De Pinto, V., Messina, A., Lane, D. J., and Lawen, A. (2010) Voltage-dependent anion-selective channel (VDAC) in the plasma membrane. *FEBS Lett.* **584,** 1793–1799
40. Ozawa, T., Natori, Y., Sako, Y., Kuroiwa, H., Kuroiwa, T., and Umezawa, Y. (2007) A minimal peptide sequence that targets fluorescent and functional proteins into the mitochondrial intermembrane space. *ACS Chem. Biol.* **2,** 176–186
41. Gieffers, C., Korioth, F., Heimann, P., Ungermann, C., and Frey, J. (1997) Mitofilin is a transmembrane protein of the inner mitochondrial membrane expressed as two isoforms. *Exp. Cell Res.* **232,** 395–399
42. Odgren, P. R., Toukatly, G., Bangs, P. L., Gilmore, R., and Fey, E. G. (1996) Molecular characterization of mitofilin (HMP), a mitochondria-associated protein with predicted coiled coil and intermembrane space targeting domains. *J. Cell Sci.* **109**, 2253–2264
43. Xie, J., Marusich, M. F., Souda, P., Whitelegge, J., and Capaldi, R. A. (2007) The mitochondrial inner membrane protein mitofilin exists as a complex with SAM50, metaxins 1 and 2, coiled-coil-helix coiled-coil-helix domain-containing protein 3 and 6, and DnaJC11. *FEBS Lett.* **581,** 3545–3549